BEILSTEIN JOURNAL OF ORGANIC CHEMISTRY

Supporting Information

for

Effect of substitution position of aryl groups on the thermal back reactivity of aza-diarylethene photoswitches and prediction by density functional theory

Misato Suganuma, Daichi Kitagawa, Shota Hamatani and Seiya Kobatake

Beilstein J. Org. Chem. **2025,** *21,* 242–252. doi:10.3762/bjoc.21.16

Experimental details and analyses of thermal back reactions

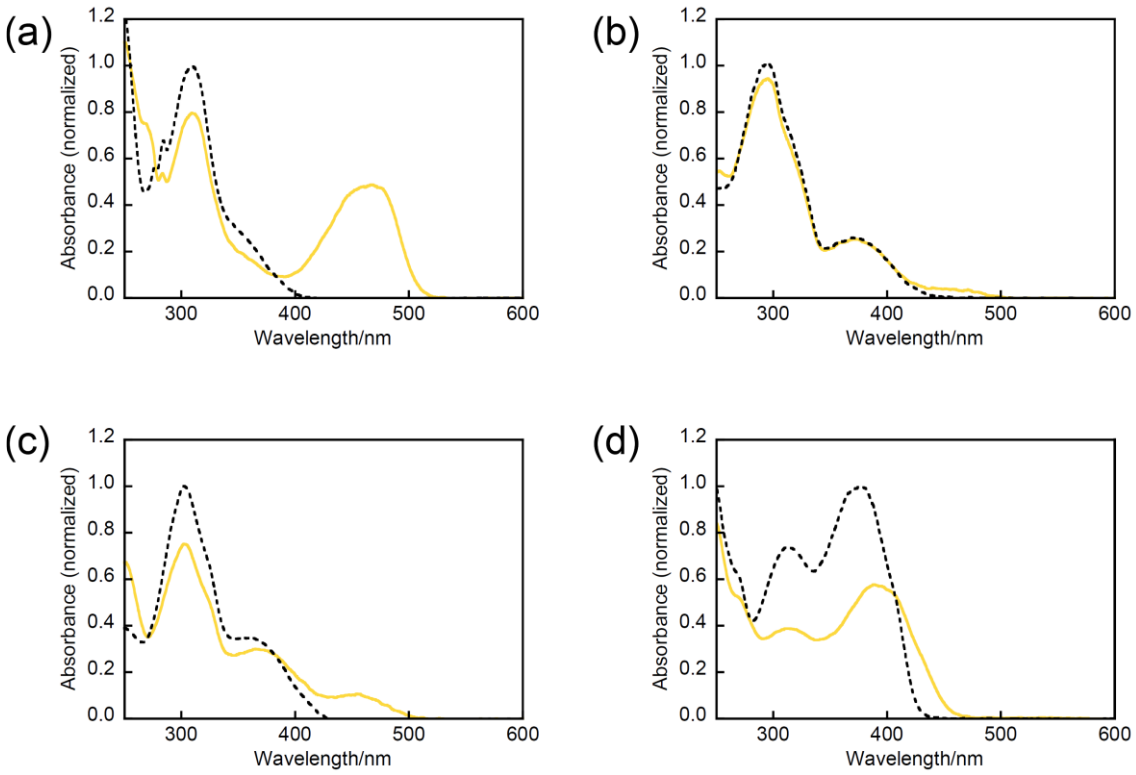

Figure S1. Absorption spectral changes of (a) **N4**, (b) **I1**, (c) **I2**, and (d) **I4** in *n*-hexane at 253 K for **N4**, 188 K for **I1**, 248 K for **I2**, and 233 K for **I4**: open-ring isomer (black line) and under irradiation with 365 nm light (yellow line).

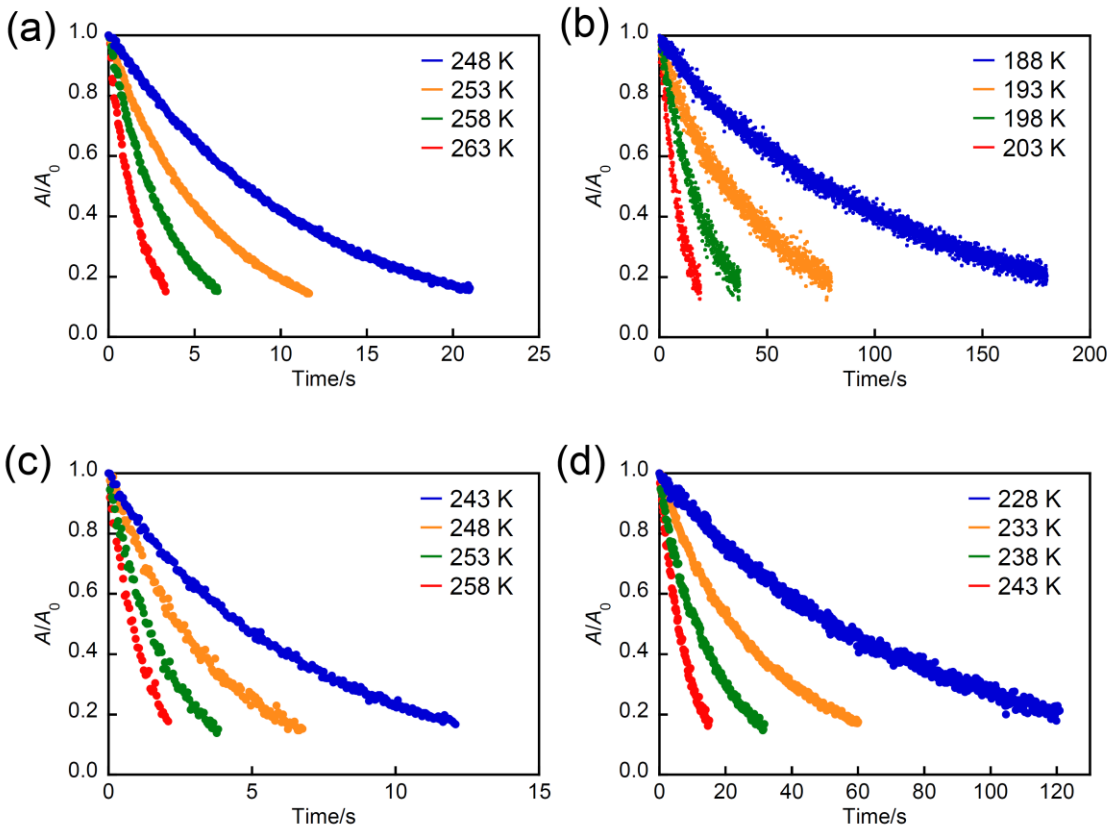

Figure S2. Absorbance decay curves at λ_{max} for the closed-ring isomer of (a) **N4**, (b) **I1**, (c) **I2**, and (d) **I4** in *n*-hexane at various temperatures.

Kinetic analysis of thermal back reaction

The reaction kinetics of the thermal back reaction were analyzed in a manner similar to a procedure from [S1]. If the thermal back reaction from the closed-ring isomer to the open-ring isomer obeys a first-order kinetics, the kinetic equation is expressed as following equation by using Lambert–Beer law.

$$\ln\frac{A_t}{A_0} = -kt$$

where k is the reaction rate constant, t is reaction time, and A_0 and A_t are absorbance of the closed-ring isomer at initial state (t = 0 s) and at arbitrary reaction time t, respectively. The k value can be calculated from the slope of the linear plot. The calculated k values are summarized in Tables S1–S6.

Eyring equation can be described as follows.

$$\ln(\frac{k}{T}) = -\frac{\Delta H^{\ddagger}}{R}\frac{1}{T} + \ln(\frac{k_B}{h}) + \frac{\Delta S^{\ddagger}}{R}$$

where R is gas constant, and T is absolute temperature, $\Delta H^{\ddagger}$ is enthalpy of activation, $\Delta S^{\ddagger}$ is entropy of activation, h is Planck constant, and k_B is Boltzmann constant. The linear relationship can be obtained by plotting $\ln(k/T)$ relative to $1/T$ as shown in Figures 2c, 2f, and S4. The $\Delta H^{\ddagger}$ and $\Delta S^{\ddagger}$ values can be determined from the slope and intercept of the linear plot. The Gibbs energy of activation ($\Delta G^{\ddagger}$) was also determined using the relationship of $\Delta G^{\ddagger} = \Delta H^{\ddagger} - T\Delta S^{\ddagger}$. The results are summarized in Table 1.

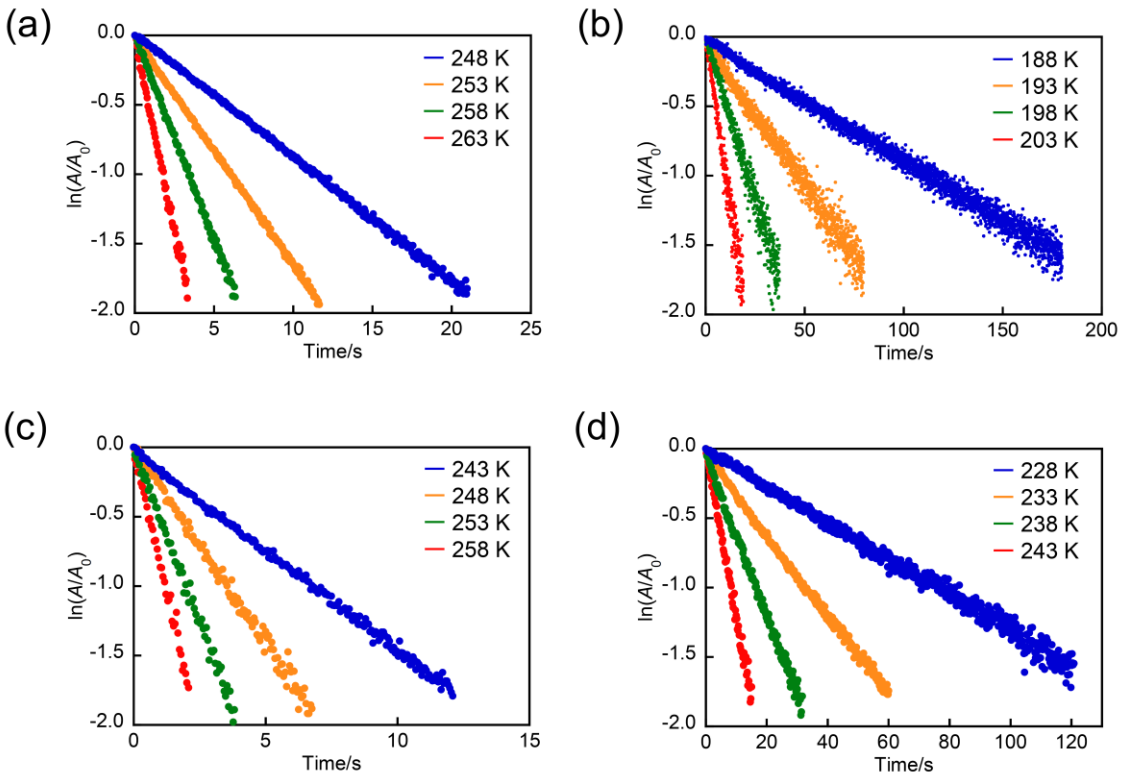

Figure S3. First-order kinetics profiles of (a) **N4**, (b) **I1**, (c) **I2**, and (d) **I4** in *n*-hexane at various temperatures.

Table S1. First-order rate constants for the thermal back reaction of **N3**.

T/K	k/s^{-1}
268.15	2.7786
263.15	1.6819
258.15	0.99070
253.15	0.58548
248.15	0.33166

Table S2. First-order rate constants for the thermal back reaction of **N4**.

T/K	k/s^{-1}
263.15	0.56137
258.15	0.29591
253.15	0.16604
248.15	0.088796

Table S3. First-order rate constants for the thermal back reaction of **I1**.

T/K	k/s^{-1}
203.15	0.096947
198.15	0.047296
193.15	0.021232
188.15	0.0088692

Table S4. First-order rate constants for the thermal back reaction of **I2**.

T/K	k/s^{-1}
258.15	0.82360
253.15	0.50140
248.15	0.28179
243.15	0.14671

Table S5. First-order rate constants for the thermal back reaction of **I3**.

T/K	k/s^{-1}
218.15	0.23092
213.15	0.11483
208.15	0.046481
203.15	0.020947

Table S6. First-order rate constants for the thermal back reaction of **I4**.

T/K	k/s^{-1}
243.15	0.12016
238.15	0.059738
233.15	0.029971
228.15	0.013128

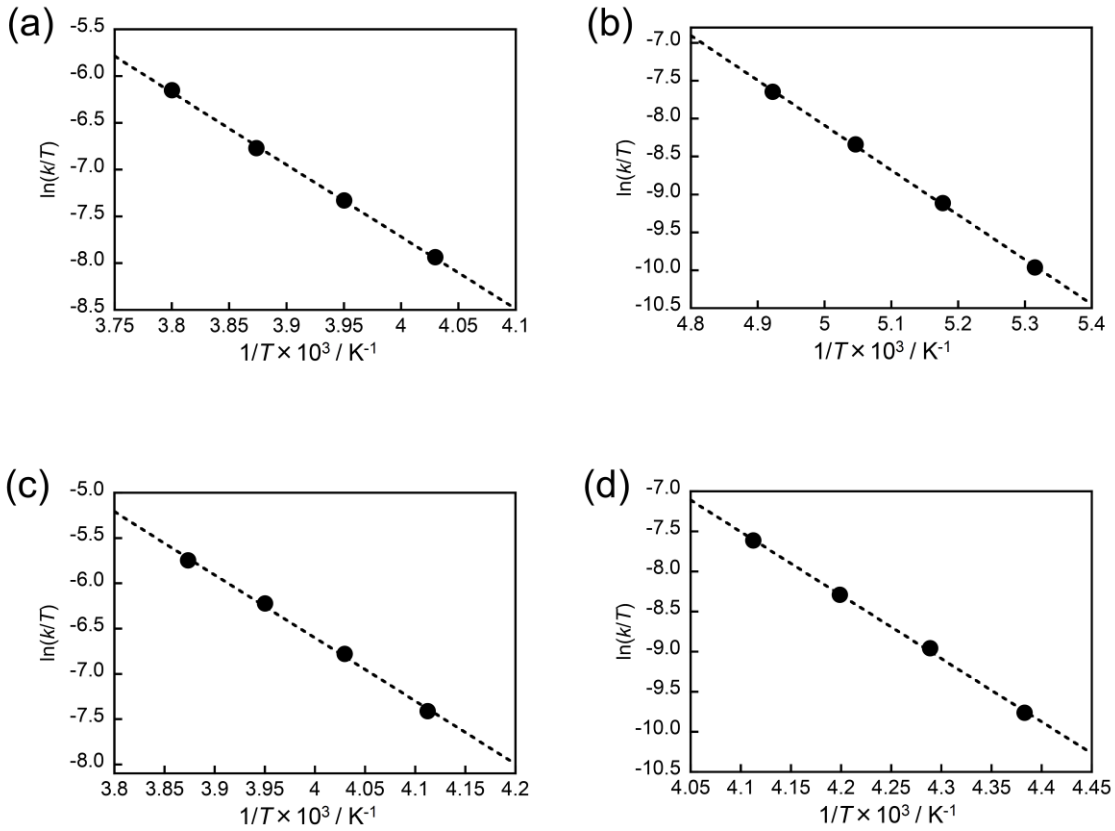

Figure S4. Temperature dependence of the rate constant (k) for the thermal back reaction of (a) **N4**, (b) **I1**, (c) **I2**, and (d) **I4**.

Table S7. $\Delta G^{\ddagger}_{(calcd)}$ values for the thermal back reaction of **N1** calculated by various functionals.

Functional	Energy(closed)/hartree	Energy(TS)/hartree	$\Delta G^{\ddagger}_{(calcd)}$/kJ mol^{-1}
B3LYP	−2219.850078	−2219.830002	52.70954201
BMK	−2218.878913	−2218.850459	74.70598269
CAMB3LYP	−2219.25252	−2219.226836	67.43334714
M05	−2219.11833	−2219.098226	52.78305602
M06	−2219.034041	−2219.010424	62.00643822
M05-2x	−2219.705172	−2219.679122	68.39428021
M06-2x	−2219.268477	−2219.242634	67.85080167
MPW1PW91	−2219.555087	−2219.531743	61.28967667
ωB97X-D	−2219.401133	−2219.374696	69.41034879

Table S8. $\Delta G^{\ddagger}_{(calcd)}$ values for the thermal back reaction of **N2** calculated by various functionals.

Functional	Energy(closed)/hartree	Energy(TS)/hartree	$\Delta G^{\ddagger}_{(calcd)}$/kJ mol^{-1}
B3LYP	−2235.909998	−2235.888727	55.84701476
BMK	−2234.943358	−2234.913817	77.55990141
CAMB3LYP	−2235.314216	−2235.28719	70.95676841
M05	−2235.184903	−2235.163601	55.92840526
M06	−2235.096344	−2235.071147	66.15472854
M05-2x	−2235.762666	−2235.734993	72.65546703
M06-2x	−2235.326503	−2235.299103	71.93870548
MPW1PW91	−2235.610396	−2235.585645	64.98375545
ωB97X-D	−2235.455080	−2235.427073	73.53238410

Table S9. $\Delta G^{\ddagger}_{(calcd)}$ values for the thermal back reaction of **N3** calculated by various functionals.

Functional	Energy(closed)/hartree	Energy(TS)/hartree	$\Delta G^{\ddagger}_{(calcd)}$/kJ mol^{-1}
B3LYP	−2142.473906	−2142.452865	55.24314971
BMK	−2141.560936	−2141.531075	78.40006147
CAMB3LYP	−2141.926479	−2141.899096	71.89407198
M05	−2141.807472	−2141.786641	54.69179467
M06	−2141.720812	−2141.697114	62.21910374
M05-2x	−2142.340784	−2142.313707	71.09066892
M06-2x	−2141.930246	−2141.903082	71.31908743
MPW1PW91	−2142.198475	−2142.174382	63.25617632
ωB97X-D	−2142.054623	−2142.026967	72.61083353

Table S10. $\Delta G^{\ddagger}_{(calcd)}$ values for the thermal back reaction of **N4** calculated by various functionals.

Functional	Energy(closed)/hartree	Energy(TS)/hartree	$\Delta G^{\ddagger}_{(calcd)}$/kJ mol^{-1}
B3LYP	−1819.501278	−1819.480961	53.34228756
BMK	−1818.684947	−1818.657711	71.50812345
CAMB3LYP	−1818.940022	−1818.913564	69.46548429
M05	−1818.809089	−1818.789033	52.65703201
M06	−1818.748308	−1818.725300	60.40750860
M05-2x	−1819.379875	−1819.352976	70.62332988
M06-2x	−1818.963865	−1818.937695	68.70934023
MPW1PW91	−1819.200959	−1819.177167	62.46590076
ωB97X-D	−1819.076335	−1819.049735	69.83830532

Table S11. $\Delta G^{\ddagger}_{(calcd)}$ values for the thermal back reaction of **I1** calculated by various functionals.

Functional	Energy(closed)/hartree	Energy(TS)/hartree	$\Delta G^{\ddagger}_{(calcd)}$/kJ mol^{-1}
B3LYP	−2219.837618	−2219.822445	39.83671
BMK	−2218.867411	−2218.843667	62.33988
CAMB3LYP	−2219.242852	−2219.220579	58.47777
M05	−2219.108242	−2219.092197	42.12615
M06	−2219.022557	−2219.004122	48.40110
M05-2x	−2219.695076	−2219.672165	60.15284
M06-2x	−2219.258380	−2219.235792	59.30480
MPW1PW91	−2219.543017	−2219.524413	48.84481
ωB97X-D	−2219.392333	−2219.368678	62.10621

Table S12. $\Delta G^{\ddagger}_{(calcd)}$ values for the thermal back reaction of **I2** calculated by various functionals.

Functional	Energy(closed)/hartree	Energy(TS)/hartree	$\Delta G^{\ddagger}_{(calcd)}$/kJ mol^{-1}
B3LYP	−2235.909189	−2235.890671	48.61901
BMK	−2234.942664	−2234.914845	73.03879
CAMB3LYP	−2235.316345	−2235.290497	67.86393
M05	−2235.186029	−2235.166787	50.51987
M06	−2235.096425	−2235.074298	58.09444
M05-2x	−2235.763844	−2235.738292	67.08678
M06-2x	−2235.327432	−2235.301752	67.42285
MPW1PW91	−2235.609811	−2235.587721	57.99730
ωB97X-D	−2235.457182	−2235.430100	71.10380

Table S13. $\Delta G^{\ddagger}_{(calcd)}$ values for the thermal back reaction of **I3** calculated by various functionals.

Functional	Energy(closed)/hartree	Energy(TS)/hartree	$\Delta G^{\ddagger}_{(calcd)}$/kJ mol^{-1}
B3LYP	−2142.462843	−2142.447063	41.43039
BMK	−2141.550084	−2141.526487	61.95393
CAMB3LYP	−2141.916587	−2141.893481	60.66481
M05	−2141.798519	−2141.781101	45.73096
M06	−2141.711411	−2141.691621	51.95865
M05-2x	−2142.331467	−2142.307798	62.14296
M06-2x	−2141.921024	−2141.897261	62.38976
MPW1PW91	−2142.188328	−2142.168441	52.21332
ωB97X-D	−2142.046331	−2142.021823	64.34576

Table S14. $\Delta G^{\ddagger}_{(calcd)}$ values for the thermal back reaction of **I4** calculated by various functionals.

Functional	Energy(closed)/hartree	Energy(TS)/hartree	$\Delta G^{\ddagger}_{(calcd)}$/kJ mol^{-1}
B3LYP	−1819.480062	−1819.461538	48.63477
BMK	−1818.665876	−1818.638035	73.09655
CAMB3LYP	−1818.920004	−1818.893345	69.99321
M05	−1818.788685	−1818.768481	53.04561
M06	−1818.72886	−1818.706397	58.97661
M05-2x	−1819.359613	−1819.332649	70.79399
M06-2x	−1818.944392	−1818.917309	71.10642
MPW1PW91	−1819.180423	−1819.157921	59.07901
ωB97X-D	−1819.058532	−1819.030614	73.29871

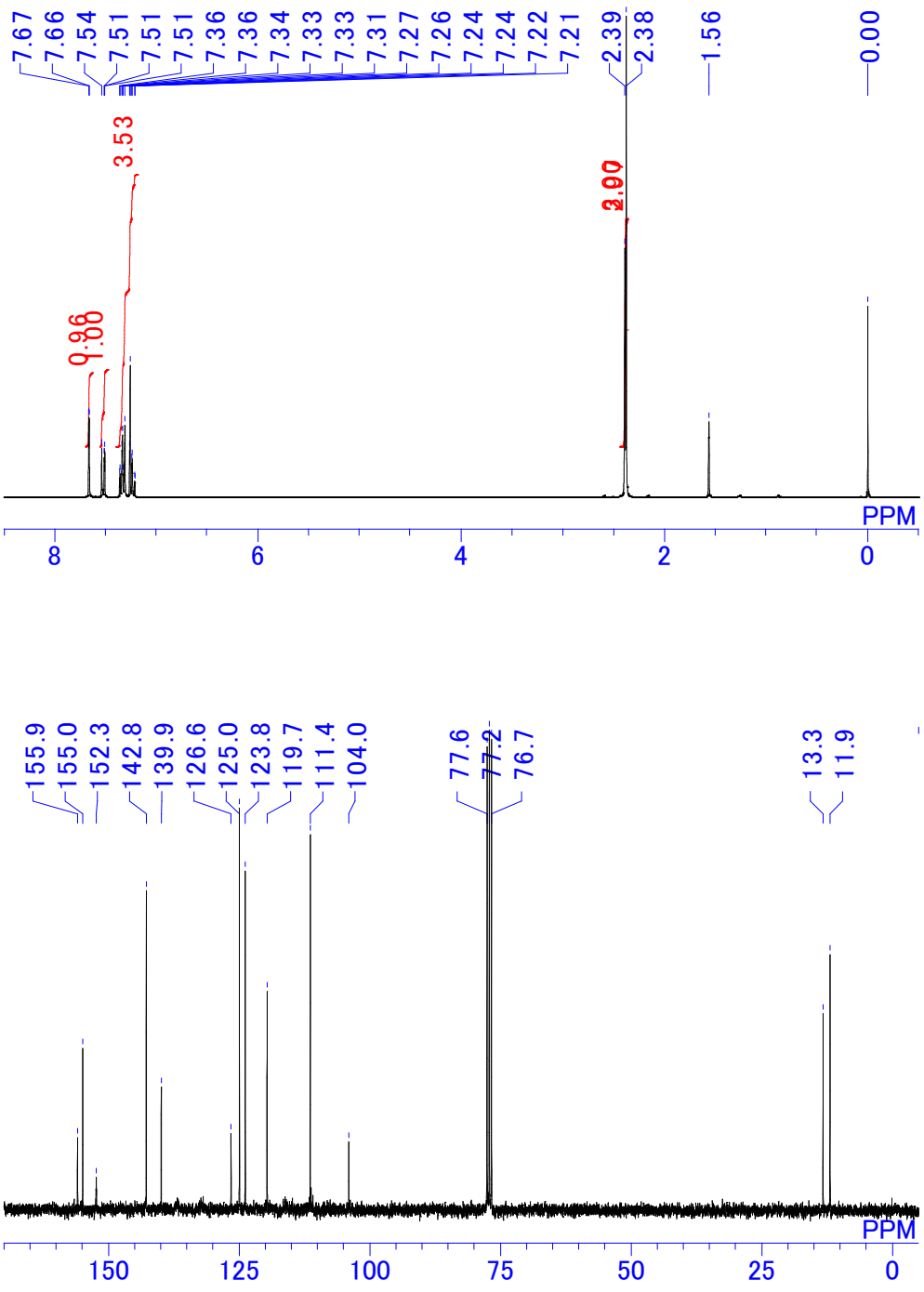

Figure S5. ^{1}H NMR and ^{13}C NMR spectra for the open-ring isomer of **N4** in $CDCl_3$.

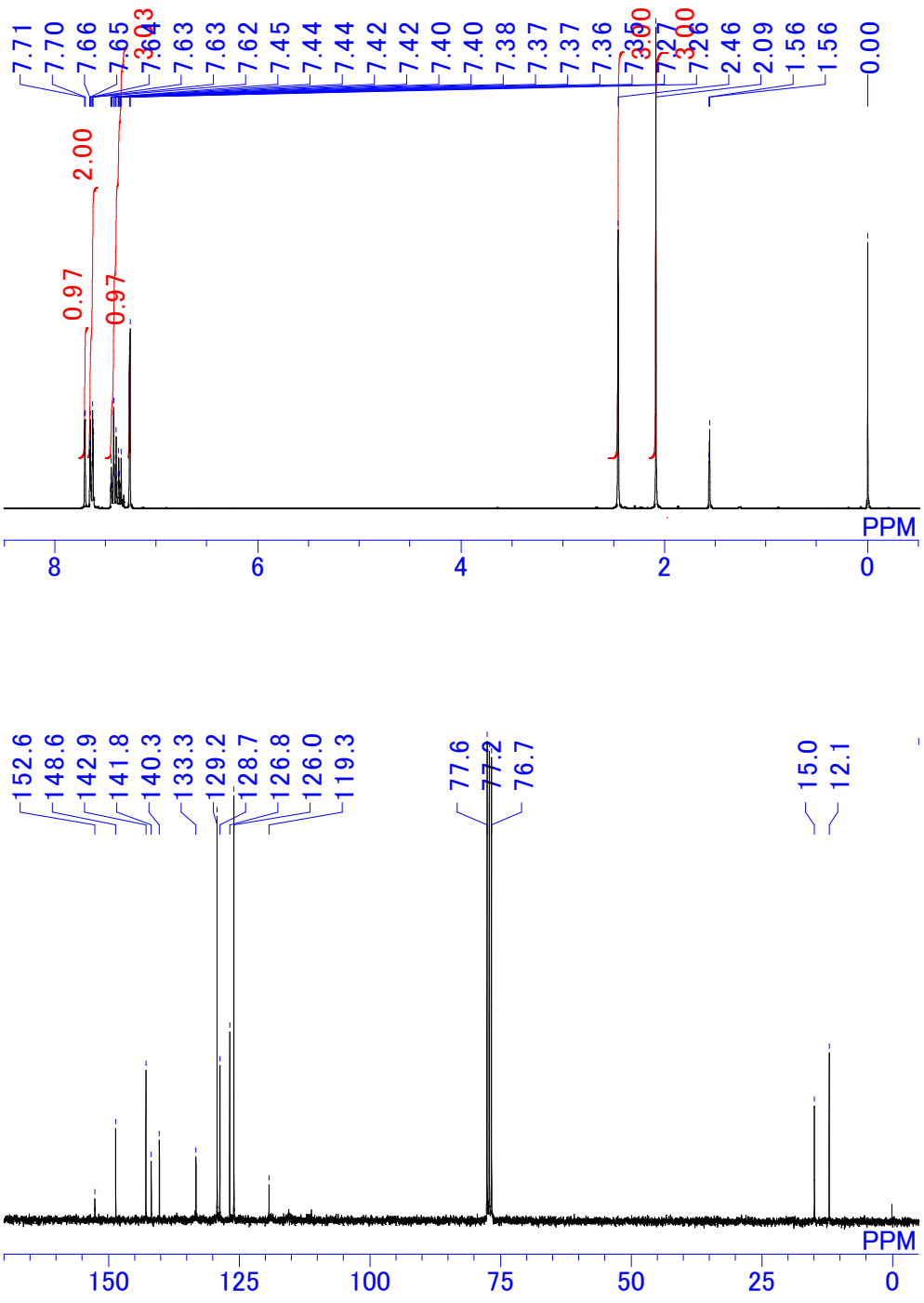

Figure S6. ^{1}H NMR and ^{13}C NMR spectra for the open-ring isomer of **I1** in $CDCl_3$.

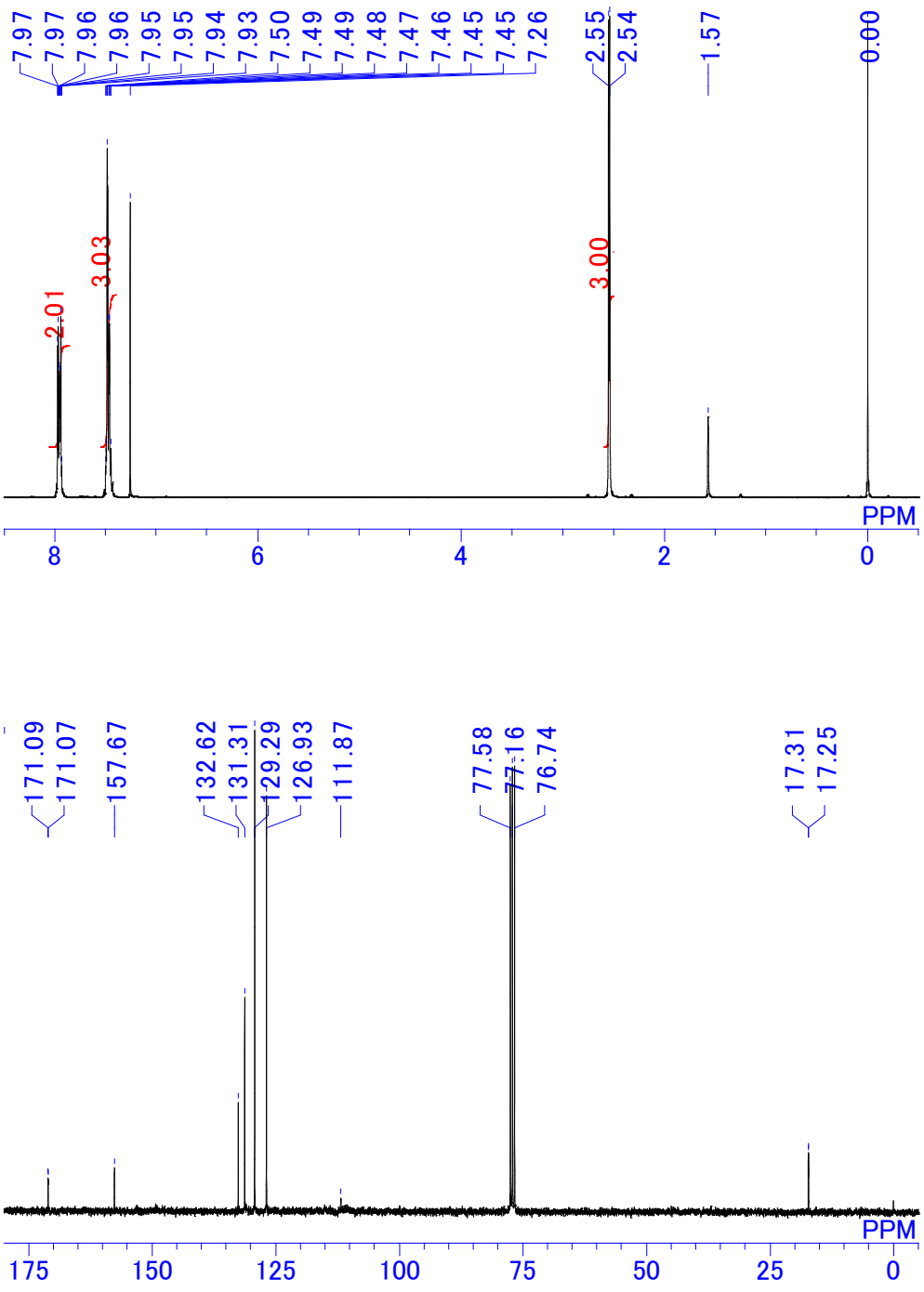

Figure S7. ^{1}H NMR and ^{13}C NMR spectra of **I2(a)** in $CDCl_3$.

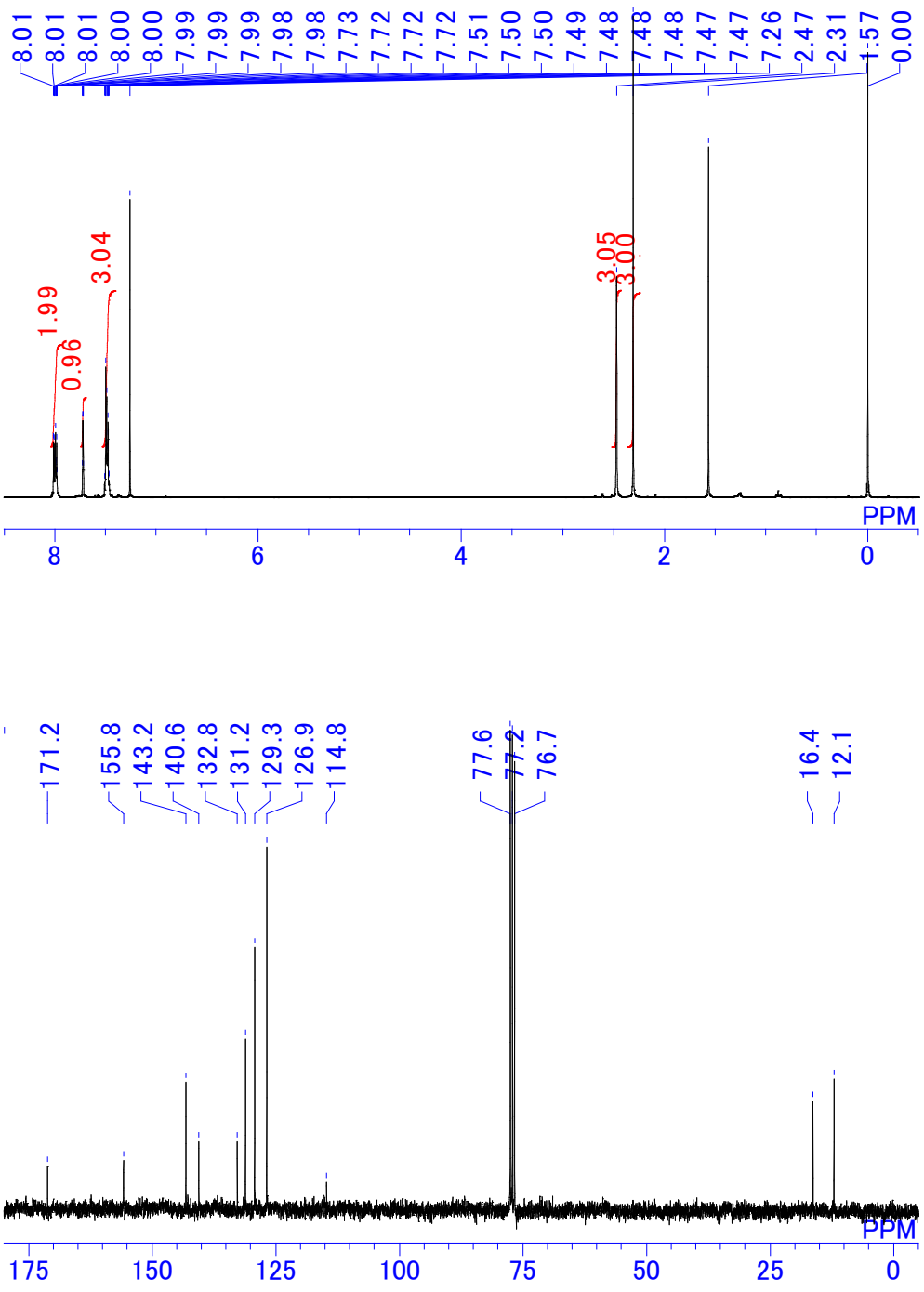

Figure S8. ^{1}H NMR and ^{13}C NMR spectra for the open-ring isomer of **I2** in $CDCl_3$.

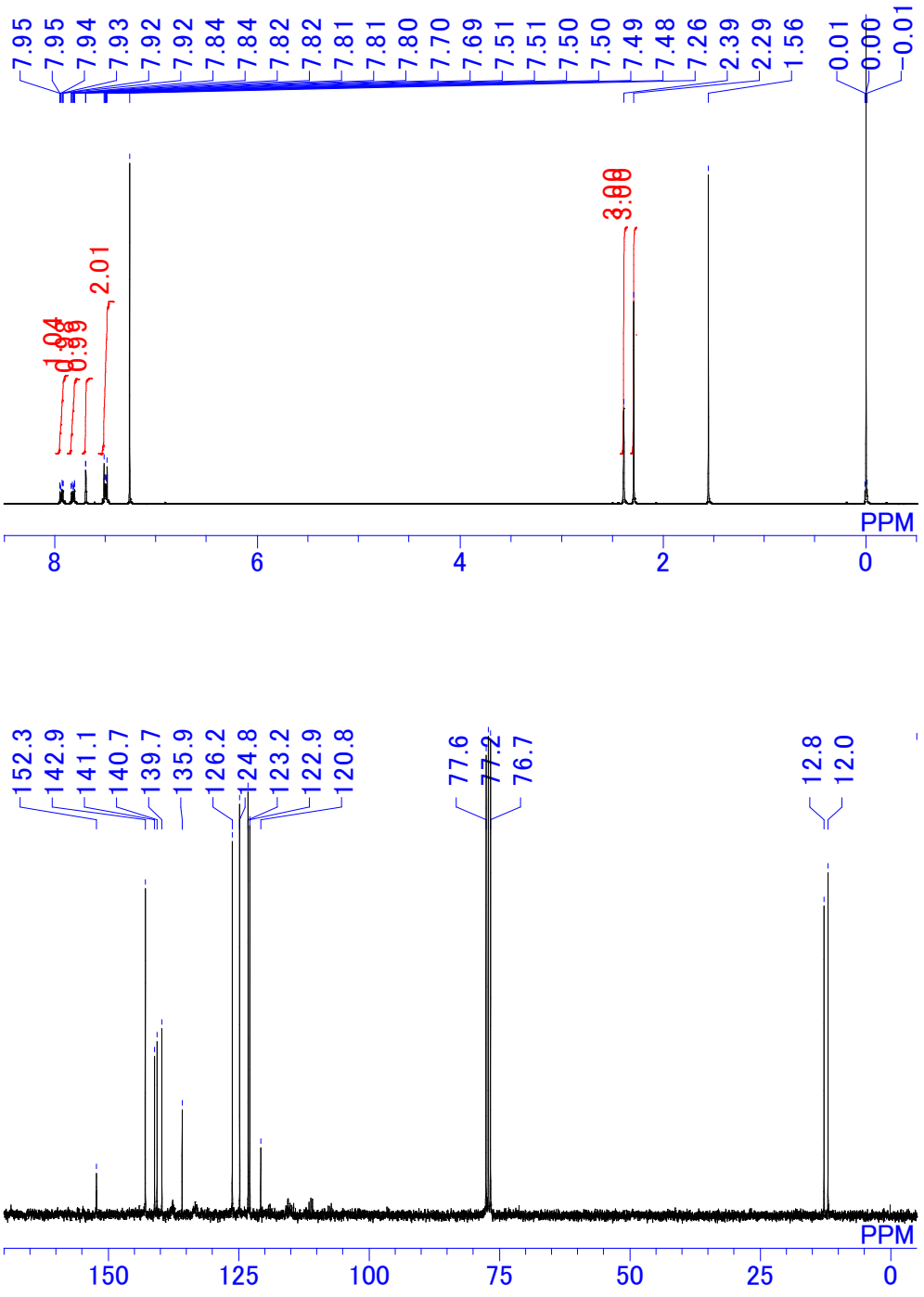

Figure S9. ^{1}H NMR and ^{13}C NMR spectra for the open-ring isomer of **I3** in $CDCl_3$.

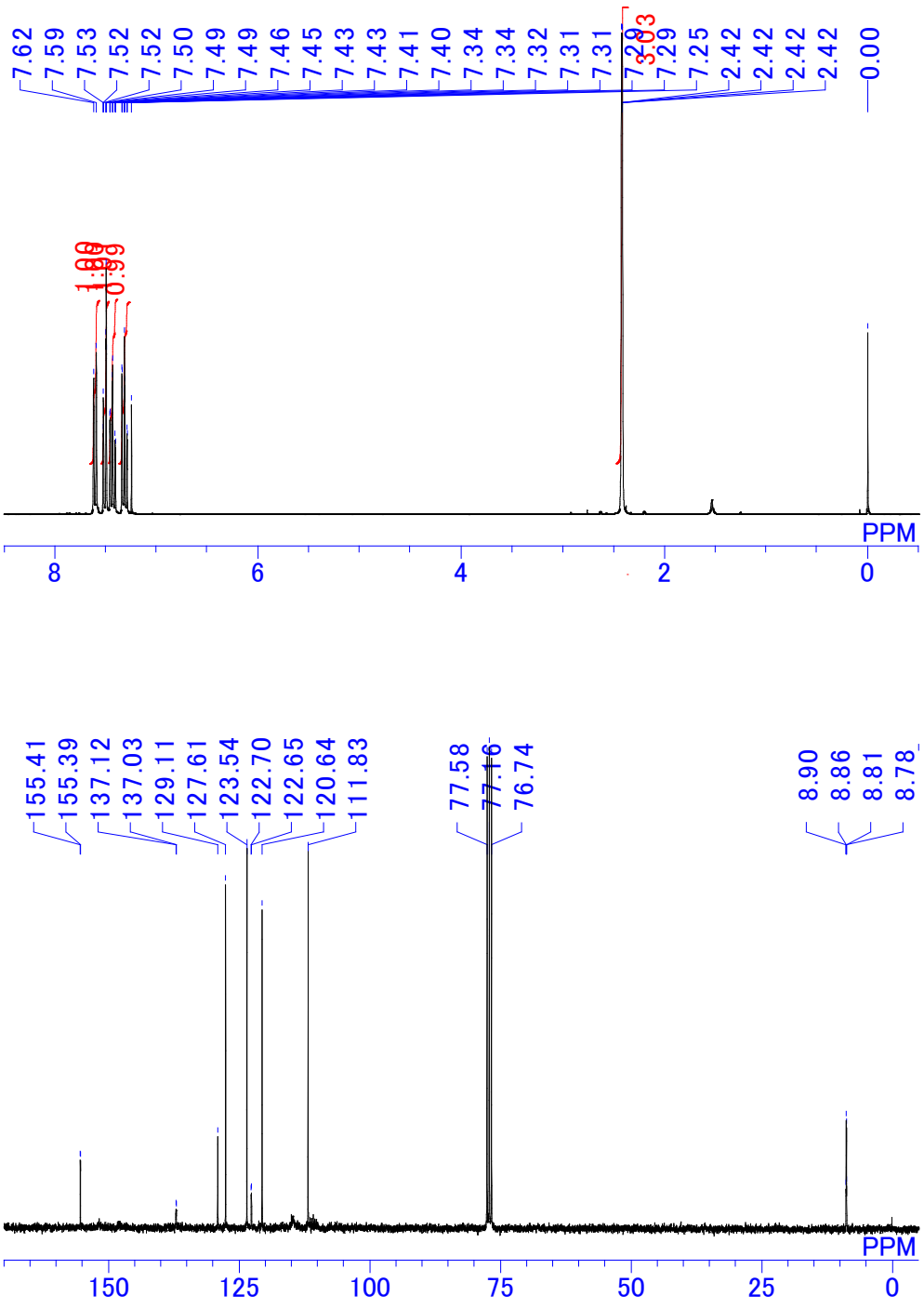

Figure S10. ^{1}H NMR and ^{13}C NMR spectra of **I4(a)** in $CDCl_3$.

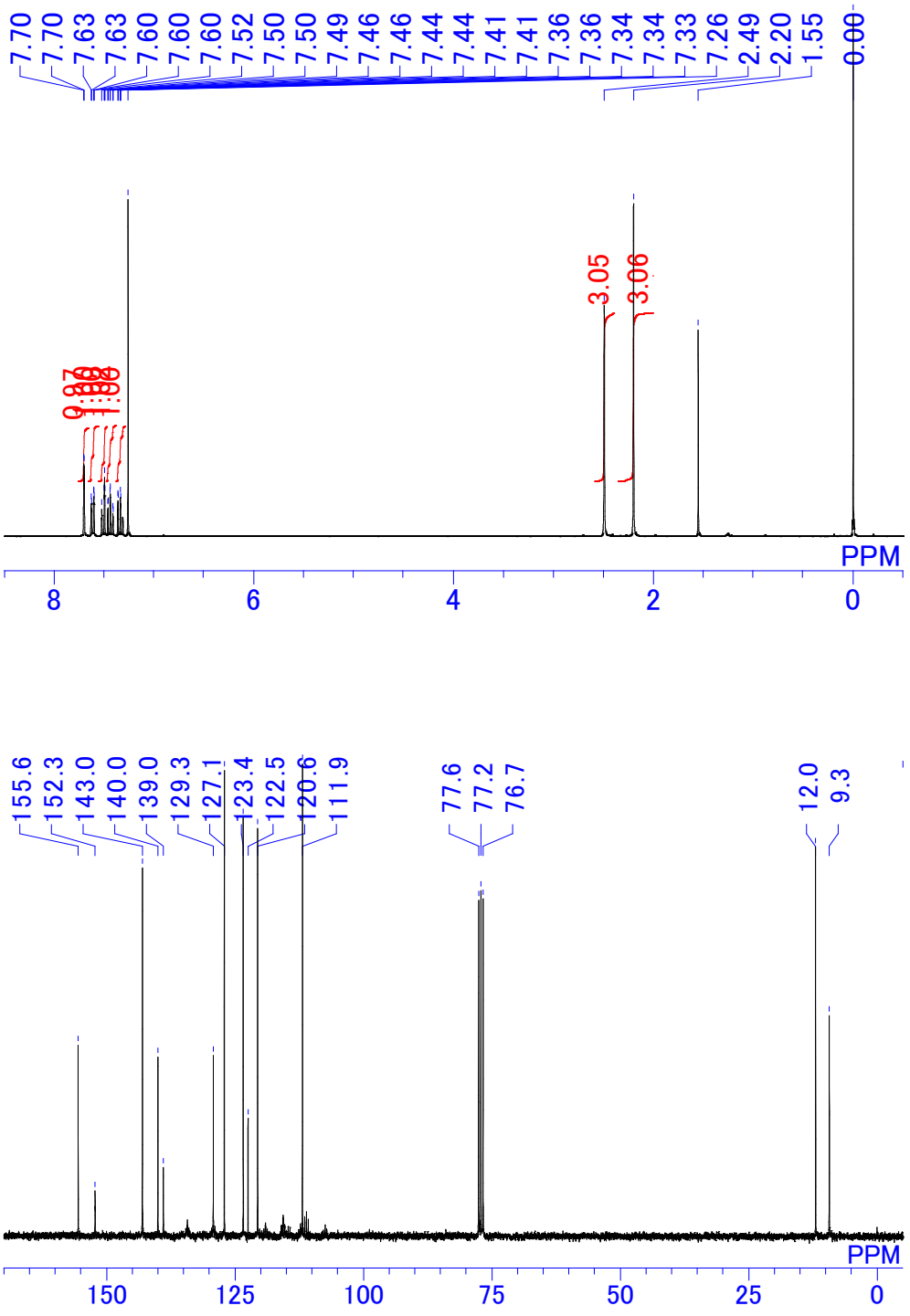

Figure S11. ^{1}H NMR and ^{13}C NMR spectra for the open-ring isomer of **I4** in $CDCl_3$.

References

(S1) Kitagawa, D.; Takahashi, N.; Nakahama, T.; Kobatake, S. *Photochem. Photobiol. Sci.* **2020**, *19*, 644–653. doi:10.1039/d0pp00024h